Strong Energy Dependence of the Optical Potential for $^{32}S+^{58,64}Ni$ near the Coulomb Barrier

A. M. Stefanini, D. Bonamini, A. Tivelli, G. Montagnoli, G. Fortuna, and Y. Nagashima[a]
Istituto Nazionale di Fisica Nucleare, Laboratori Nazionali di Legnaro, I-35020 Legnaro, Italy

S. Beghini and C. Signorini
Dipartimento di Fisica, Università di Padova, and Istituto Nazionale di Fisica Nucleare, Padova, Italy

A. DeRosa, G. Inglima, and M. Sandoli
Dipartimento di Fisica, Università di Napoli, and Istituto Nazionale di Fisica Nucleare, Napoli, Italy

and

G. Cardella and F. Rizzo
Dipartimento di Fisica, Università di Catania, and Istituto Nazionale di Fisica Nucleare, Catania, Italy
(Received 24 September 1987)

The elastic scattering of $^{32}S+^{58,64}Ni$ was measured at sulfur beam energies of 82, 88, 91, 93, 98, 102.5, 108, and 150 MeV. Evidence is found for a marked energy dependence of the optical potential at the strong-absorption radii around the Coulomb barrier, in good agreement with parallel information extracted from the fusion cross sections for the same systems.

PACS numbers: 25.70.Cd

The observed enhancements and anomalies of the heavy-ion fusion cross sections at subbarrier energies[1] have triggered a number of theoretical and experimental investigations[2] about the competing quasielastic reaction channels in the same energy range. In fact, the behavior of those channels seems to determine the subbarrier fusion probabilities to a large extent in many cases (see Refs. 1 and 2 for recent reviews). A renewed and correlated interest[3,4] about heavy-ion elastic scattering has grown as a result of the evidence of rapid variations of the optical potential with energy[5-8] near to the top of the Coulomb barrier. A rapid variation of the imaginary part (caused by the closing of the nonelastic channels) is predicted[5] to lead to a corresponding variation of the real part. This increases the attraction of the nuclear surfaces (polarization) in that range of energies, thereby enhancing the subbarrier fusion. An early analysis of similar spirit was performed by Delagrange, Vaz, and Alexander[9] $^{16}O+^{208}Pb$. There a substantial strengthening of the real (proximity) potential was found necessary to fit the fusion and elastic-scattering data at energies close to the barrier, whereas only small adjustments of the potential were sufficient at higher energies.

We felt that it was important to obtain more experimental data in this respect, as the evidence for the so-called "threshold anomaly" of the optical potential is restricted to a few cases, some of which are reanalyses of old experiments. In fact the only clear-cut evidence, if we restrict ourselves to heavy-ion collisions, comes from $^{16}O+^{208}Pb$.[3,9] We chose the systems $^{32}S+^{58,64}Ni$, where the previous measurements of fusion[10] and quasielastic transfer[11] cross sections provide us with a rather complete knowledge of the relevant reaction channels at near-barrier energies. The evidence from those experiments is also that both subbarrier fusion and nucleon transfer are largely favored for $^{32}S+^{64}Ni$ in comparison to $^{32}S+^{58}Ni$. The Coulomb barriers[12] are 89.4 and 94.2 MeV, respectively, in the laboratory frame.

The present elastic-scattering measurements were performed with the ^{32}S beam from the Legnaro XTU Tandem accelerator, at energies of 82, 88, 91, 93, 98, 102.5, 108, and 150 MeV. The $^{58,64}Ni$ targets were 30 $\mu g/cm^2$ thick, evaporated onto 20-$\mu g/cm^2$ carbon backings. They were 99.8% and 96.7% enriched in mass 58 and 64, respectively. A 50-cm-diam sliding-seal scattering chamber was used. Two forward-placed Si detectors monitored the beam intensity. The elastically scattered sulfur ions were detected and identified by means of three time-of-flight energy telescopes employing microchannel plates (start) and 200–300-mm^2 silicon surface-barrier detectors (stop and energy signals) over a flight path of 80–100 cm. Mass and energy resolutions were $A/\Delta A \simeq 50$ and $\Delta E \simeq 700$–800 keV FWHM. The angular distributions could be measured as far back as $\theta_{c.m.} \simeq 160°$. A maximum angular uncertainty $\Delta\theta_{lab} \simeq \pm 0.25°$ has been estimated, including mechanical as well as beam-focusing contributions. In addition, an integration over $\pm 0.30°$–$0.45°$ occurred as a result of the finite beam spot and detector size.

The data are shown in Figs. 1 and 2 together with the fits obtained with the optical-model code PTOLEMY.[13] At the lowest measured energies large-angle structures show up in the angular distributions; they are indicative of deviations from the "normal" strong-absorption conditions, and forced us to introduce a surface imaginary potential besides the volume-absorbing Woods-Saxon po-

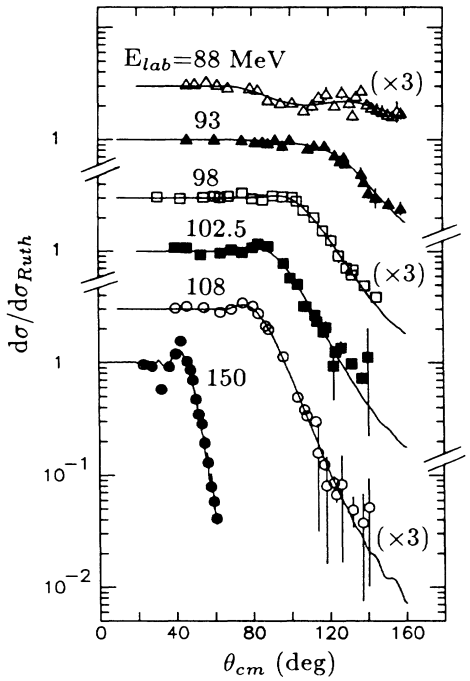

FIG. 1. Elastic-scattering angular distributions for ^{32}S + ^{58}Ni at different laboratory energies (not corrected for target thickness). The solid lines are optical-model fits obtained with the code PTOLEMY (Ref. 13).

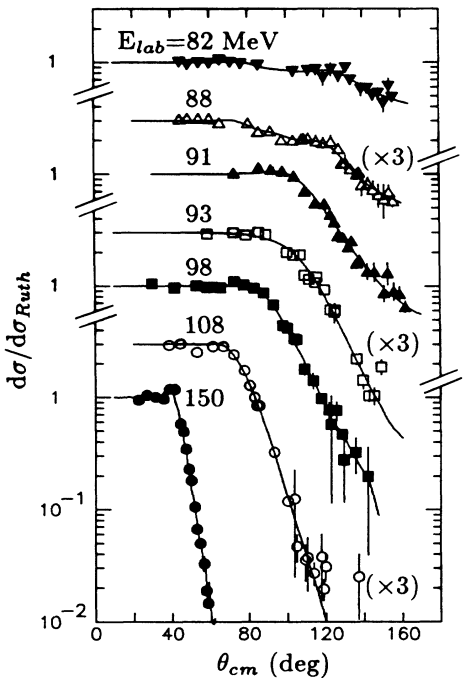

FIG. 2. Same as Fig. 1 but for ^{32}S+^{64}Ni.

tential in order to obtain acceptable fits. The underlying and probably interesting physics is still under investigation but, anyway, outside the object of this Letter. At these low energies no reliable determination of the potentials around the strong-absorption radii can be done, also in view of the fact that, apart from 88-MeV ^{32}S+^{64}Ni, no quarter-point angle is observed in the angular distributions.

Good fits could be obtained for the higher-energy angular distributions by our varying the parameters of a standard Woods-Saxon potential. Systematic searches were done at every energy for both systems; as an example of this analysis, Table I reports eight different potentials for 98-MeV ^{32}S+^{64}Ni. In some of them, an identical geometry was used for the real and imaginary parts and/or one or more parameters were kept fixed. The three-parameter fit of set 8 is more than acceptable; it uses $R_0 = R_{i0} = 1.247$ fm, i.e., the grand average of the radius parameters obtained in sets 3, 4, 5, 6 for all energies of that system.

Table II lists the best-fit parameters obtained when we fixed the real well depth and the reduced radii in this way. The strong-absorption radii (from the quarter-point recipe) do not vary significantly with the energy, as expected ($r_{sa} = 10.8 \pm 0.1$ fm for ^{32}S+^{58}Ni and $r_{sa} = 11.2 \pm 0.1$ fm for ^{32}S+^{64}Ni). In a narrow range

TABLE I. Optical-model parameters resulting from different fits to the data for the system 98-MeV ^{32}S+^{64}Ni. Italicized values were kept fixed, and pairs of parameters marked with the same symbol were kept equal.

Set	V (MeV)	R_0 (fm)	a (fm)	W (MeV)	R_{i0} (fm)	a_i (fm)	χ^2_{pt}	σ_{reac} (mb)
1	72.2	1.304	0.39*	124.2	1.307	0.39*	1.07	584
2	44.2	1.342°	0.38*	81.3	1.342°	0.38*	1.01	582
3	55.9	1.188	*0.63*	26.5	1.399	0.37	1.42	565
4	24.4	1.265°	*0.63*	153.0	1.265°	0.42	0.93	570
5	55.1	1.232	*0.55*	57.7	1.342	0.40	1.14	574
6	26.2	1.296°	*0.55*	151.0	1.296°	0.39	1.02	571
7	16.4	*1.247*	0.83	112.8	*1.247*	0.45	0.91	555
8	*50.0*	*1.247*	0.55	303.7	*1.247*	0.40	1.11	574

TABLE II. Optical-model parameters resulting from three-parameter fits to the elastic-scattering data. The fixed parameters were $V=50$ MeV and $R_0=R_{i0}=1.247$ fm. The bombarding energies are corrected for target thickness.

System	E_{lab} (MeV)	a (fm)	W (MeV)	a_i (fm)	χ^2_{pt}	σ_{reac} (mb)
$^{32}S+^{64}Ni$	90.3	0.64	397	0.34	1.88	270
	92.8	0.53	13.0	0.76	2.59	504
	97.3	0.55	304	0.40	1.11	574
	107.3	0.48	88.0	0.51	1.31	941
	149.4	0.55	35.5	0.56	1.11	1709
$^{32}S+^{58}Ni$	92.8	0.58	4.52	0.84	0.72	221
	97.3	0.57	241	0.34	0.91	275
	101.8	0.54	304	0.35	3.53	436
	107.3	0.53	189	0.36	1.24	575
	149.4	0.57	130	0.35	5.21	1371

around those internuclear distances the potential is rather unambiguously determined by the data. The corresponding values of the real and imaginary potentials are shown in Fig. 3, as derived from the three-parameter fits of Table II and the error bars cover the fit uncertainties.

The real potential shows a rapid increase as the energy approaches the barrier and a corresponding decrease of the absorption is observed. This trend does not change qualitatively when plotting the potentials derived from other fits of the data (e.g., Table I).

Also reported in Fig. 3 are the values of the real potential resulting from the fusion[10] data and the barrier-penetration model (BPM).[5,14] The basic assumption underlying this model is that the fusion of two nuclei at near-barrier or subbarrier energies takes place after the penetration of a one-dimensional potential barrier. It has been pointed out[14] that the BPM should be able to give reliable predictions of the fusion cross sections, provided the potential is given a suitable energy dependence. Inversely, we extract the potential needed in the BPM to reproduce the fusion data at each measured energy with some assumptions about the potential shape. We have used a sharp imaginary potential confined within the barrier and deep enough to ensure complete absorption of the ingoing flux: In practice these conditions were met with $W=10$ MeV, $R_{i0}=1.0$ fm, and $a_i=0.25$ fm. The real reduced radii were fixed at 1.25 fm, the real diffusenesses were the average values resulting from the fits of the elastic-scattering data (Table II), and the well depth V was varied to achieve agreement between the calculated reaction cross section and the measured fusion cross section. The errors quoted in Fig. 3 only reflect the experimental uncertainties in the fusion cross sections.

The "fusion" potentials shown in Fig. 3 are in good agreement with the values derived from the present elastic-scattering measurements. This is an excellent proof that the BPM correctly describes the average effect of the many competing quasielastic reaction channels on

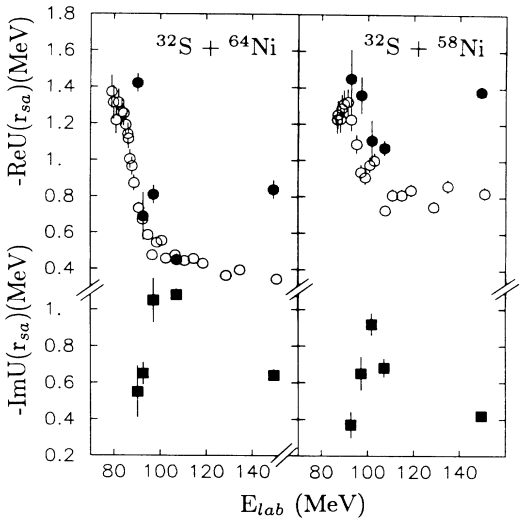

FIG. 3. The real and imaginary parts of the optical potential evaluated at the strong-absorption radii vs the bombarding energy [$r_{sa}=10.8$ (11.2) fm for $^{32}S+^{58(64)}Ni$, respectively]. The filled symbols are derived from the present elastic-scattering experiments and the open circles from the older fusion data (Ref. 10).

the fusion cross sections at and below the Coulomb barrier (some problem is visible for the 150-MeV data, as may be expected far above the barrier where the BPM is inadequate). A marked energy dependence of the real potential around the Coulomb barrier is shown by the fusion data, the effect being much more conspicuous for $^{32}S+^{64}Ni$ which has, in fact, subbarrier fusion cross sections a factor of 10 larger[10] than the other system.

In summary, we have presented the results of elastic-scattering measurements in $^{32}S+^{58,64}Ni$ at various energies around the Coulomb barrier. Large-angle structures in the angular distributions are systematically observed at the lowest measured energies. The data were analyzed within the optical model, and the optical potential turns out to be strongly energy dependent in the vicinity of the barrier, as evidenced also by a BPM analysis of previous fusion cross-section experiments for the same systems. More generally, the present elastic-scattering data are essential to indicate experimentally how such quantities like the amount of subbarrier fusion, transfer yield, surface transparency or absorption, and ion-ion potential strength at grazing distances are tied together and determine the reaction mechanism of heavy ions at low energies.

[a]On leave from University of Tsukuba, Tsukuba, Japan.

[1]M. Beckerman, Phys. Rep. **129**, 145 (1985).

[2]K. E. Rehm, in Proceedings of the Symposium on The Many Facets of Heavy-Ion Fusion Reactions, Argonne National Laboratory, Illinois, March 1986, Report No. ANL-PHY-

86-1 (to be published), p. 27.

[3]J. S. Lilley *et al.*, Phys. Lett. **151B**, 181 (1985).

[4]E. Vulgaris *et al.*, Phys. Rev. C **33**, 2017 (1986).

[5]M. A. Nagarajan, C. C. Mahaux, and G. R. Satchler, Phys. Rev. Lett. **54**, 1136 (1985); C. Mahaux, H. Ngo, and G. R. Satchler, Nucl. Phys. **A449**, 354 (1986).

[6]I. J. Thompson *et al.*, Phys. Lett. **157B**, 250 (1985).

[7]S. C. Pieper, M. J. Rhoades-Brown, and S. Landowne, Phys. Lett. **162B**, 55 (1985).

[8]B. R. Fulton *et al.*, Phys. Lett. **162B**, 55 (1985).

[9]H. Delagrange, L. C. Vaz, and J. M. Alexander, Phys. Rev. C **20**, 1731 (1979).

[10]A. M. Stefanini *et al.*, Nucl. Phys. **A456**, 509 (1986).

[11]A. M. Stefanini *et al.*, Phys. Lett. B **185**, 15 (1987).

[12]L. C. Vaz, J. M. Alexander, and G. R. Satchler, Phys. Rep. **69**, 373 (1981).

[13]M. H. Macfarlane and S. C. Pieper, Argonne National Laboratory Report No. ANL-76-11 (Revision 1), 1978 (unpublished); M. J. Rhoades-Brown, S. C. Pieper, and M. H. Macfarlane, Phys. Rev. C **21**, 2417 (1980).

[14]M. A. Nagarajan and G. R. Satchler, Phys. Lett. B **173**, 29 (1986).